DEUTSCHES ELEKTRONEN-SYNCHROTRON DESY

DESY 86-139
November 1986

QCD AND HEAVY QUARK PHYSICS AT LEP AND SLC

by

A. Ali

Deutsches Elektronen-Synchrotron DESY, Hamburg

ISSN 0418-9833

NOTKESTRASSE 85 · 2 HAMBURG 52

To be sure that your preprints are promptly included in the HIGH ENERGY PHYSICS INDEX , send them to the following address (if possible by air mail) :

DESY
Bibliothek
Notkestrasse 85
2 Hamburg 52
Germany

DESY 86-139
November 1986

ISSN 0418-9833

QCD and Heavy Quark Physics at LEP and SLC *

A. Ali

Deutsches Elektronen-Synchrotron DESY,
Hamburg, Federal Republic of Germany

Abstract

Some selected applications of perturbative Quantum Chromodynamics, QCD, in e^+e^- annihilation physics for the ongoing PETRA/PEP experiments and the forthcoming LEP/SLC experiments are discussed. In the second half of this report some aspects of heavy quark physics, involving production and decays of bottom and top quarks are reviewed. We particularly emphasize experimental measurements leading to the determination of the Cabibbo-Kobayashi-Maskawa matrix elements V_{bu}, V_{ts} and V_{td}.

* Talks given at the 14th International Winter Meeting on Fundamental Physics, St. Feliu, Spain, March 1986.

Introduction

Electron positron annihilation processes have proven time and again their invaluable worth as precision tools available in high energy physics experiments. The large investments made in the construction of the Large Electron Positron storage ring, LEP, at CERN, and the Stanford Linear Collider, SLC, at SLAC are evidence of the commitment and trust in e^+e^- machines, shown by very large sections of high energy physics community. Let us hope that the new machines will fulfil their promise by adding new glorious chapters to the continuing saga of success, which many of us have witnessed at earlier e^+e^- machines, SLAC, DORIS, CESR, PEP and PETRA.

The physics of the pre-LEP/SLC era in e^+e^- annihilation has been dominated by vector bosons. They have been observed both directly, like ρ, φ, J/ψ, Υ, and indirectly, like the virtual Z^0 boson whose effects have been seen clearly through the increase in the total hadronic cross-section at PETRA, and in electroweak charge asymmetries. Likewise, the vector bosons of QCD, gluons, were discovered in e^+e^- annihilation by the observation of three-jet events [1]. The dominance of vector bosons in e^+e^- data is not to be confused with the statement that e^+e^- annihilation physics itself can be understood or explained by the so-called vector dominance models! As we are going to describe in detail below, hadronic final states in e^+e^- annihilation are readily explained in terms of QCD. In fact, they have provided some of the most quantitative and trustworthy tests of perturbative QCD, known so far [2]. As higher beam energies and statistics become available, it will be possible at LEP and SLC to sharpen some of the tests already carried out at lower energies. Surely, more tests will be thought of and carried through. The role of QCD is also destined to change qualitatively

from the one of a candidate theory of strong interactions to the one of the standard description, which will be used to estimate "usual backgrounds" for non-standard phenomena. The present consensus on the standard description of hadronic final states holds at the perturbative level only. A standard theory of non-perturbative phenomena has not yet evolved [3].

Lest I be misunderstood, I must hasten to add that there are some noble exceptions to the simple minded generalization that e^+e^- physics has been dominated by vector bosons, two of which stand out, according to my taste and judgement, above the "usual background", seen everyday in high energy physics experiments. The exceptions are the discovery of the $\tau^{\pm}$ lepton by Martin Perl and his collaborators at SLAC [4], and the unexpectedly long lifetime of the botton hadrons, measured at PEP and PETRA [5]. Needless to say that the standard model of electroweak interactions [6] would have remained incomplete without the third generation of leptons. The relatively long lifetime of bottom hadrons is a boon in disguise, the actual beneficiaries of which will be experiments dedicated to the study of bottom physics. Since, in the standard model, Z^0 decays about 15 % of the time in the $b\bar{b}$ final state, and the anticipated cross section at the Z^0 peak, $\sigma(e^+e^- \rightarrow Z^0)$, is estimated to be O(30 nb), one has potential bottom factories at the Z^0 peak in the form of LEP and SLC machines. This is a good reason why the subject of bottom hadron physics deserves some attention at LEP and SLC.

The traditional course of e^+e^- machines, as precision tools in the study of the standard physics of vector bosons, will be set forth at LEP and SLC. It is not difficult to foresee three nearby main "stations" of the "e^+e^- train", namely the Z^0 peak, the toponia resonances and the W^+W^- threshold region. The central issue for experiments at LEP and SLC to address is to unravel the mechanism

of spontaneous symmetry breaking, generically called the Higgs mechanism [7]. A related issue at LEP II is to confirm the non-abelian $W^+W^-Z^0$ coupling of the standard model [8]. These topics, however, by no means exhaust the potential of LEP physics, which even in a conservative scenario has many more interesting facets to offer. I will restrict myself to the discussion of some selected topics in applications of QCD in e^+e^- annihilation, and review some aspects of heavy quark physics at LEP and SLC.

It is not easy to find novel tests of QCD in e^+e^- physics. This is so because e^+e^- annihilation has been a traditional and popular area for the application of perturbative QCD ideas [9]. There is, however, a quantitative difference between the energy scales at LEP/SLC and e^+e^- physics at lower energies. This would allow kinematic reconstruction of multijet states, in particular 4-jet and 5-jet states in the production processes $e^+e^- \rightarrow \gamma^*, Z^0, \theta \rightarrow$ hadrons. In addition, the event rate at the Z^0 peak, with the estimated cross-sections $\sigma(Z^0) \simeq 30$ nb, is expected to be large, yielding several million Z^0 events at LEP in a typical year. The study of multijet final states in $e^+e^- \rightarrow$ n jets, with $n \geqslant 4$ is an obvious field of research at LEP and SLC, where detailed tests of QCD would be undertaken. At PETRA energies, clear evidence of 4 jet events has been seen in a number of experiments [10]. While these experiments are certainly adequate in supplying an existence proof for 4-jets, they lack the statistics to undertake more detailed and precise tests. Since in e^+e^- annihilation, the full non-abelian gauge structures, involving trilinear and quadrilinear gluon couplings, are accessible directly only in $n \geqslant 4$ jet processes, $e^+e^- \rightarrow q\bar{q}gg$ and $e^+e^- \rightarrow q\bar{q}ggg$, the experiments at LEP and SLC with their large event rates are expected to provide new quantitative tests of the non-abelian nature of QCD. We illustrate such tests in Section 2 by showing examples from the decays

$Z^0 \rightarrow$ 4 jets, and $\theta \rightarrow$ 4 jets, γ + 3 jets [11]. No calculations for $e^+e^- \rightarrow$ 5 jets exist yet, except in the trivial leading log form [12], and hence detailed discussions involving the quadrilinear gluon coupling will have to be postponed for the time being. Judging from the recent jet analysis at PETRA and the rapid rise in jet multiplicity, it is easy to make a firm prediction, namely that a detailed quantitative analysis of the LEP/SLC experiments will necessitate calculations of order α_s^3 contributions, if not of the next higher order! The field of perturbative QCD computations is still far from being exhausted!!

The second, and the larger part of this writeup concerns production and decays of heavy quarks, particularly the bottom and top quarks [13]. In the bottom sector, study of rare processes is especially important. Examples of such processes are the Cabibbo-Kobayashi-Maskawa (CKM) [14] suppressed transitions $b \rightarrow u x$, B^0-$\bar{B}^0$ oscillations [15], flavour changing neutral current processes $b \rightarrow (d,s)\ell^+\ell^-$ [16] and CP-violation [17]. All these processes provide non-trivial tests of the standard theory of flavour mixing. More specifically, they provide information on the CKM matrix elements V_{bu} (through e.g. the decay $B^0 \rightarrow \pi^+ \ell^- \bar{\nu}_\ell$), V_{ts} (from B_s^0-$\bar{B}_s^0$ mixing), V_{td} (from B_d^0 - $\bar{B}_d^0$ mixing) and the KM phase, δ, from eventual CP violation measurements in the bottom sector. The last three of the aforementioned measurements involve higher order (loop) contributions in the standard model and hence they provide a window on the more distant particle physics landscape, which may reveal the existence of new forces or matter.

The other interest in Z^0 decays in the context of heavy quark physics lies in the possibility of observing $Z^0 \rightarrow t\bar{t}$ final state. Since estimates of the branching ratio $BR(Z^0 \rightarrow t\bar{t})$ are of order 3 % for $m_t \lesssim 40$ GeV, (see below), the

$Z^0 \rightarrow t\bar{t}$ decays may be the most copious source of top quarks in high energy experiments for some time to come. For $m_t > m_{z/2}$, the $t\bar{t}$ state would be produced in the continuum at LEP, though the rate would be much lower. The first point to confirm in top quark physics, apart from a precise determination of m_t, would be to check if the top quark indeed belongs to the standard model $SU(2)_L$ doublet. Another interesting question to investigate concerns the measurements of the CKM matrix elements V_{tb}, V_{ts} and V_{td}. This, however, due to the overwhelming dominance of the V_{tb} matrix element, is going to be a formidable proposition [19]. As pointed out earlier, observations of $B_d^0 \leftrightarrow \bar{B}_d^0$ and $B_s^0 \leftrightarrow \bar{B}_s^0$ transitions also provide alternative measurements of the CKM matrix elements V_{td} and V_{ts}. We shall review present bounds on these matrix elements [18]. Section 4 contains a summary and an outlook.

2. Application of QCD in e^+e^- annihilation

We briefly review here some known and well established, and some yet to be tested, aspects of perturbative QCD in e^+e^- annihilation. The topics that are discussed here include the determination of the total hadronic cross section, also expressed in terms of the ratio $R \equiv \frac{\sigma(e^+e^- \rightarrow \text{hadrons})}{\sigma(e^+e^- \rightarrow \mu^+\mu^-)}$, and the top quark mass effects in the top quark pair production threshold region. Also discussed are present determination of $\alpha_s(Q^2)$ at PETRA and PEP, expectations at LEP and techniques to measure directly the non-abelian gluon couplings at the Z^0 and toponium resonances. Since detailed discussions and formalism of all these topics have been documented in LEP reports [19] and published literature, we shall not attempt to be self contained and avoid going into technical details here.

2.1 Hadronic cross sections and the branching ratios $Z^0 \to f\bar{f}$

It is well known that at PETRA/PEP energies, the total hadronic cross section in the quark-parton model (i.e. without QCD corrections) has the expression

$$\sigma_0 = \sum_q \sigma_q \left(1 - \frac{\pi G_F}{\sqrt{2}\alpha} \frac{V_e V_q}{Q_q (1 - s/m_Z^2)}\right) \qquad (2.1)$$

$$\sigma_q = \frac{4\pi\alpha^2}{s} Q_q^2 \quad , \quad s = E_{cm}^2$$

where Q_q, V_q and V_e are the electric charge of the quarks, quark vector couplings and the vector couplings of the electron, respectively. In the standard model the vector and axial vector couplings are given by

$$a_e = a_{(d,s,b)} = -a_{(u,c,t)} = -0.5$$

$$v_e = (4 \sin^2\theta_w - 1) \simeq -0.04$$

$$v_{(d,s,b)} = -1/2 + 2/3 \sin^2\theta_w \simeq -0.347$$

$$v_{(u,c,t)} = 1/2 - 4/3 \sin^2\theta_w \simeq 0.193 \qquad (2.2)$$

where we have also given numerical values for $\sin^2\theta_w = 0.23$.

Perturbative QCD corrections to σ_0 have been known for quite some time. The result, in the so-called $\overline{MS}$ scheme [20], can be expressed as [21]

$$\sigma = \sigma_0 \left(1 + \frac{\alpha_s(Q^2)}{\pi} + C_2 \left(\frac{\alpha_s(Q^2)}{\pi}\right)^2\right) \qquad (2.3)$$

$$\alpha_s(Q^2) = \frac{12\pi}{(33 - 2n_q)\ln(Q^2/\Lambda^2)} \left[1 - \frac{3(306 - 38n_q)}{(33 - 2n_q)^2} \times \frac{\ln\ln(Q^2/\Lambda^2)}{\ln(Q^2/\Lambda^2)}\right]$$

The expressions (2.1)-(2.3) show that a precise measurement of the total hadronic cross-section σ can determine both $\sin^2\theta_w$ and $\alpha_s(Q^2)$. Recent attempts using PETRA/PEP data, shown in fig. 1, give at Q = 34 GeV, [22]

$$\alpha_s(Q^2) = 0.17 \pm 0.03$$

$$\sin^2\theta_w = 0.24 \pm 0.02 \qquad (2.4)$$

The errors in (2.4) are dominated by systematics, a good part of which is due to theoretical uncertainty from $O(\alpha^4)$ QED corrections, which have not yet been completely calculated.

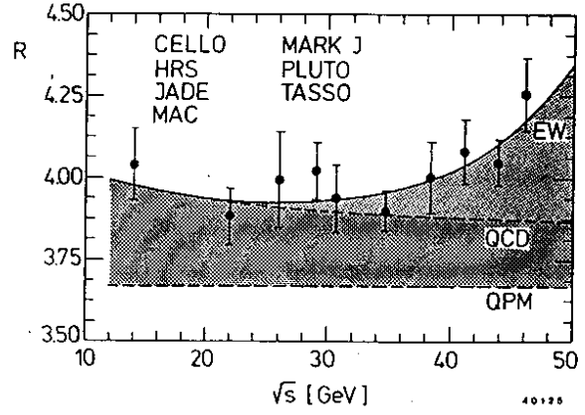

Fig. 1. The hadronic total cross section R and the fitted contributions of QCD and the electroweak interaction (from Ref. (22))

Let us now discuss the changes that a shift to the energy region $s \simeq m_Z^2$ would entail. The first change is in the expression for σ_o, which at the Z^o pole is given by

$$\sigma_o = \sum_q \frac{G_F^2 m_Z^4}{2\pi \Gamma_Z^2} \left(V_e^2 + a_e^2 \right)\left(V_q^2 + a_q^2 \right) \qquad (2.5)$$

where Γ_Z is the Z^o decay width. If one ignores the quark masses, which is an excellent approximation for the first five quarks at LEP energies, then the QCD corrections given in (2.3) also hold at the Z^o peak. The large value of m_t, however, introduces non-trivial changes. If $m_t > m_{Z/2}$, then production of top quark is kinematically forbidden and the measurement of the total hadronic cross-sections at the Z^o peak will provide very precise measurements of $\sin^2\theta_w$ and $\alpha_s(Q^2)$ at LEP/SLC energies. The remark made earlier about the importance of $O(\alpha^4)$ QED corrections applies here as well.

The effects of m_t for hadronic cross-section enter in two ways. First, it is well known that the velocity dependent corrections for both $\sigma(e^+e^- \to t\bar{t})$ near threshold and the partial decay width $\Gamma(Z^o \to t\bar{t})$ are not small. Secondly, it is conceivable that the toponium ($t\bar{t}$) states turn out to be almost degenerate in mass with the Z^o boson. In that case, one expects a fascinating pattern of γ Z, θ, interferences near the Z^o peak [23]. Such interferences, while changing the θ decays completely, could also have non-negligible effects for σ.

The QCD and velocity dependent corrections for σ can be succintly expressed at $s \simeq m_Z^2$ as follows

$$\sigma\,(t\bar{t}) = R_V^t \sigma_{VV}^t + R_A^t \sigma_{AA}^t \qquad (2.6)$$

with

$$\sigma_{VV}^t = \frac{G_F^2 m_Z^4}{2\pi \Gamma_Z^2} \left(V_e^2 + a_e^2 \right) V_t^2$$
$$\sigma_{AA}^t = \frac{G_F^2 m_Z^4}{2\pi \Gamma_Z^2} \left(V_e^2 + a_e^2 \right) a_t^2 \qquad (2.7)$$

The correction factors R_V^t and R_A^t are given by [24]

$$R_V^t = \frac{\beta_t (3-\beta_t^2)}{2} \left\{ 1 + \frac{4}{3}\alpha_s(Q^2) \times \left[\frac{\pi}{2\beta_t} - \left(\frac{3+\beta_t}{4} \right)\left(\frac{\pi}{2} - \frac{3}{4\pi} \right) \right] \right\}$$

$$R_A^t = \beta_t^3 \left\{ 1 + \frac{4}{3}\alpha_s(Q^2) \left[\frac{\pi}{2\beta_t} - \left(\frac{19}{10} - \frac{22}{5}\beta_t + \frac{7}{2}\beta_t^2 \right)\left(\frac{\pi}{2} - \frac{3}{4\pi} \right) \right] \right\} \qquad (2.8)$$

with $\beta_t = (1-4m_t^2/Q^2)^{1/2}$ being the velocity of the top quark in the e^+e^- rest frame. Note that for $\beta_t \to 1$, $R_{V,A}^t \to 1$ and one recovers the massless quark expressions. One should use the same value of $\alpha_s(Q^2)$ as obtained by the extrapolation of the $n_q = 5$ expression in (2.3) to ensure continuity of $\alpha_s(Q^2)$ across the top quark threshold. The numerical importance of the threshold factors for the top quark are shown in fig. 2. The notation used in fig. 2 is such that $\gamma_{A,V} = R_{A,V}^t$ and the lowest order factors are given by the expression

$$\gamma_0^V = \beta_t (3-\beta_t^2)/2$$
$$\gamma_0^A = \beta_t^3 \qquad (2.9)$$

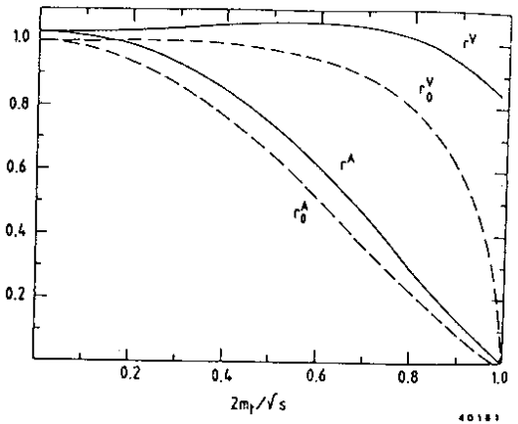

Fig. 2. Threshold factors for heavy quark production through vector and axial-vector couplings (from ref. (24))

Likewise, the velocity- and $\theta(\alpha_s)$ corrections in the partial decay rate $\Gamma(Z^0 \to t\bar{t})$ are not negligible, in case such decays are allowed kinematically. The partial rate for $\Gamma(Z^0 \to t\bar{t})$ can be expressed as

$$\Gamma(Z^0 \to t\bar{t}) = \frac{\alpha m_Z \left(R_V^t v_t^2 + R_A^t a_t^2 \right)}{4 \sin^2\theta_W \cos^2\theta_W \left(1 - \Delta r_0\right)} \qquad (2.10)$$

where Δr_0 represents the QED renormalization of the fine structure constant and numerically is estimated to be $\Delta r_0 = 0.06$ (25). The so-corrected branching ratio, $BR(Z^0 \to t\bar{t})$, is shown in fig. 3 for three representative values of m_Z and $\sin^2\theta_w$ as indicated. For $m_t < 40$ GeV, this branching ratio is expected to be in excess of 3 %.

If the toponium mass, $m(\theta)$, is very close to m_Z, then one has to solve the coupled channel problem and smear the cross-section with a smoothing function. Since this is being discussed elsewhere in these proceedings [26], I will not discuss the almost ($m_\theta \simeq m_Z$) degenerate case here. In table 1, we show the

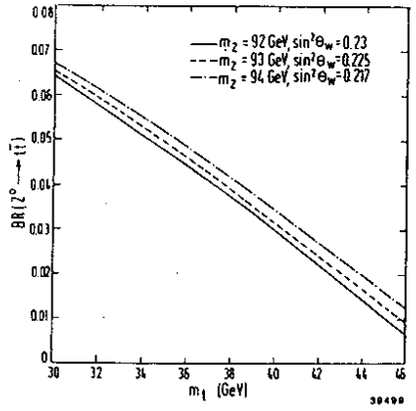

Fig. 3. The $O(\alpha_s)$ corrected branching ratio, $BR(Z^0 \to t\bar{t})$, as a function of top quark mass, values for m_Z and $\sin^2\theta_w$ as indicated (from ref. (13)).

Table 1. Branching ratios for the decays $Z^0 \to f\bar{f}$ and the Z^0 decay width including $O(\alpha)$ QED, $O(\alpha_s)$ QCD and quark mass corrections with a) m_t = 30 GeV, b) m_t = 40 GeV, c) m_t = 44 GeV

Decay Modes	BR (%) (a)	BR (%) (b)	BR (%) (c)
	6.3	6.5	6.6
$e^+e^- = \mu^+\mu^- = \tau^+\tau^-$	3.1	3.3	3.3
$d\bar{d} = s\bar{s}$	14.4	14.9	15.1
$b\bar{b}$	14.3	14.8	15.0
$u\bar{u} = c\bar{c}$	11.2	11.6	11.8
$t\bar{t}$	6.3	2.8	1.4
$\Gamma_{tot}(Z)$ GeV	2.69	2.59	2.55

2.2 Jets in e^+e^- annihilation

Ever since the discovery of quark jets by the SLAC-LBL collaboration [28] and their theoretical existence proof by Sterman and Weinberg [29], jet physics in e^+e^- annihilation and elsewhere has come a long way. This subject has been recently reviewed in ref. (11), where also references to earlier work on jet physics can be found. Leaving the details, we review here some of the salient features of jet physics at LEP energies.

The first remark concerns the determination of $\alpha_s(Q^2)$ from jets at PETRA and PEP energies. These measurements are normally done by experimentally measuring inclusive jet quantities, which are also calculable in perturbative QCD. Among the measures that have been analysed by the experimental groups at PETRA and PEP is the so-called energy-energy correlation, EEC, and in particular its asymmetry, AEEC. The EEC cross-section involves energy flow measurements in two calorimeters simultaneously and can be defined as follows

$$1/\sigma \; d^2\Sigma^{EEC}/d\Omega\, d\Omega' \equiv 1/N \sum_{a=1}^{N} \left(1/Q \; d\Sigma^a/d\Omega\right)\left(1/Q \; d\Sigma^a/d\Omega'\right) \qquad (2.11)$$

where $Q = \sqrt{s}$ is the c.m. energy, the label (a = 1 to N) refers to the specific event, out of N events, and $d\Sigma^a/d\Omega$, $d\Sigma^a/d\Omega'$ refer to the total energy deposited in each of the two calorimeters with angular segments $d\Omega$ and $d\Omega'$. The normalization is such that (including self-correlations at 0^o).

$$1/\sigma \int \left(d^2\Sigma^{EEC}/d\Omega\, d\Omega'\right) d\Omega \cdot d\Omega' = 1 \qquad (2.12)$$

Let us consider the experimental configuration, where the angle between the two calorimeters χ ($\Omega.\Omega' = \cos\chi$) and the polar angle of one of the calorimeters, measured with respect to the e^+e^- axis, θ, are fixed. This configuration is calculable in perturbative QCD. In the lowest non-trivial order, one gets

$$1/\sigma_0 \; d^2\Sigma^{EEC}/d\cos\chi\, d\cos\theta = \alpha_s(Q^2)/\pi \left[A(\xi) + \cos^2\theta\, B(\xi)\right] \qquad (2.13)$$

where $\xi = (1-\cos\chi)/2$ satisfying $0 \leq \xi \leq 1$. The functions $A(\xi)$ and $B(\xi)$ can be found in ref. (30), their explicit form is not crucial for our discussion here. Experimentalists have, however, found it convenient to integrate over θ and obtain a single differential distribution in $\cos\chi$. The "average EEC" so obtained can be expressed as

$$1/\sigma_0 \; d\Sigma^{EEC}/d\cos\chi = \alpha_s(Q^2)/\pi \; F(\xi) \qquad (2.14)$$

where $F(\xi)$ is given by [30]

$$F(\xi) = \frac{(3-2\xi)}{6\xi^5(1-\xi)}\left[2(3-6\xi+2\xi^2)\ln(1-\xi) + 3\xi(2-3\xi)\right] \qquad (2.15)$$

The AEEC cross-section has an obvious definition

$$\frac{d\Sigma^{AEEC}}{d\cos\chi} \equiv \frac{d\Sigma^{EEC}(180^o-\chi)}{d\cos\chi} - \frac{d\Sigma^{EEC}(\chi)}{d\cos\chi} = \frac{\alpha_s(Q^2)}{\pi}\left[F(1-\xi) - F(\xi)\right] \equiv \frac{\alpha_s(Q^2)}{\pi} A(\xi) \qquad (2.16)$$

The $O(\alpha_s)^2$ corrections to the averaged EEC and AEEC functions $F(\chi)$ and $A(\chi)$, respectively, have been calculated in refs. (31). Expressing these corrections as

$$\frac{1}{\sigma} d\Sigma^{EEC}/d\cos\chi = \frac{\alpha_s(Q^2)}{\pi} F(\chi)\left[1 + \frac{\alpha_s(Q^2)}{\pi} R^{EEC}(\chi)\right]$$

$$\frac{1}{\sigma} d\Sigma^{AEEC}/d\cos\chi = \frac{\alpha_s(Q^2)}{\pi} A(\chi)\left[1 + \frac{\alpha_s(Q^2)}{\pi} R^{AEEC}\right] \qquad (2.17)$$

one finds

$$R^{EEC} \simeq 9 - 12$$

$$R^{AEEC} \simeq 3 \qquad (2.18)$$

The $O(\alpha_s)^2$ contribution to the EEC cross-section is substantial ($\sim$ 40 %) but small in the AEEC ($\sim$ 10 %). The latter cross-section has been used by several groups [32] at PETRA and PEP for detailed comparison with perturbative QCD. Concentrating only on comparisons where the complete $O(\alpha_s)^2$ corrections have been implemented [33], it is fair to say that PETRA experiments find (for Q = 30-34 GeV):

$$\alpha_s(Q^2) = 0.12 \pm 0.02 \qquad (2.19)$$

which though, somewhat fragmentation model dependent, is quite consistent with the value of $\alpha_s(Q^2)$ anticipated for the QCD scale parameter, $\Lambda_{\overline{MS}}$ = 100-200 MeV. A representative result is shown in fig. 4 from which it is easy to see that the fragmentation dependence is decreasing with the increase in the center of

mass energy. It is, therefore, expected that at the much larger LEP energies, the fragmentation effects should no longer be a serious limitation in testing perturbative QCD precisely. The large statistics at the Z^0 peak would certainly be an advantage to determine the detailed profile of jets at LEP and SLC. Theoretically, if quark masses are ignored then the changes in going over from $\gamma^* \to q\bar{q}g$, $q\bar{q}gg$ to $Z^0 \to q\bar{q}g$, $q\bar{q}gg$ etc. are minimal. In any case, this machinary has been developed and can be used by our experimental colleagues.

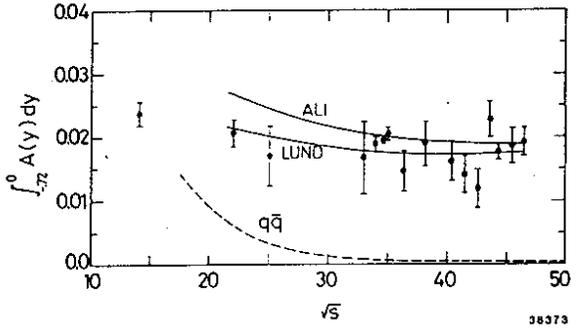

Fig. 4. The integrated AEEC cross-section measured by the MARK-J collaboration at various PETRA energies. Also shown are the fragmentation component from $e^+e^- \to q\bar{q}$ and the best fits in independent (Ali et al.) and string (Lund) fragmentation models (from ref. (34)).

2.3 Test of the nonabelian character of QCD

In this section we briefly recapitulate the tests for the nonabelian couplings in QCD suggested in the processes $e^+e^- \to \gamma$, $Z \to 4$ jets and in orthotoponium decays, $\theta \to 4$ jets, γ + 3 jets. In particular, the large event rates at the Z^0 should enable us to obtain a significant sample of 4-jet events. Moreover due to the high energy ($\sim$ 92 GeV), the separation of 4-jet events from the

more frequent 2- and 3-jet events should be lot easier than at presently available energies (29-45 GeV) at PETRA and PEP.

The 3-gluon vertex in QCD can be tested by comparing QCD with an abelian version of "QCD", in which the vector gluons carry no colour , in analogy to the photon. Quarks still appear in 3 colours in order to agree with the measured value of R. Both QCD and "QED" yield the same 3-jet rate if the couplings are related by $\alpha_{\text{"QED"}} = \frac{4}{3}\alpha_{QCD}$. In "QED", the diagram with the triple gluon coupling in fig. (5) is switched off and to be consistent, the 4-quark cross-section in $e^+e^- \to q\bar{q}q\bar{q}$ has to be multiplied by 8. This is the essential difference in the 4 jets, namely the relative contributions of the states $e^+e^- \to q\bar{q}gg$ and $e^+e^- \to q\bar{q}q\bar{q}$ in "QED" and QCD are different. Roughly speaking, in inclusive 4-jet cross sections the ratio $\sigma(q\bar{q}gg)/\sigma(q\bar{q}q\bar{q})$ is about 10 and 1 in QCD and "QED", respectively. Since the process $e^+e^- \to q\bar{q}gg$ is more singular (both in QCD and "QED") than $e^+e^- \to q\bar{q}q\bar{q}$, one expects this aspect to be emphasized lot more in QCD than in "QED" type theories. In the decays of orthotoponium, the decays $\theta \to gggg$

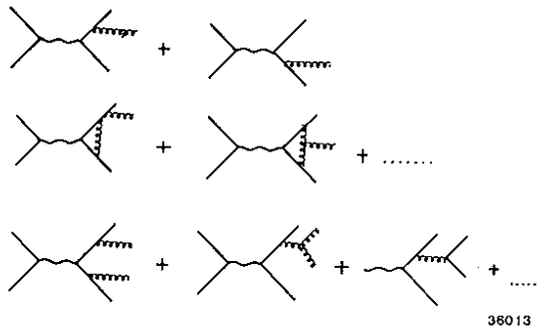

Fig. 5. Some diagrams contributing to the 3- and 4-jet processes upto $O(\alpha_s)^2$ in e^+e^- annihilation

are allowed only in QCD. However, the decays $\theta \to gg\bar{q}\bar{q}$ are allowed in both QCD and "QED". Again, the difference apart from the overall rate, lies in the intrinsic distributions in $\theta \to gggg$ decays as against the ones in $\theta \to gg\bar{q}\bar{q}$. The same qualitative statements apply to the decays $\theta \to \gamma$ + 3 jets, which in "QED" type theories arise from $\theta \to \gamma + g + q\bar{q}$.

We shall first discuss the case $e^+e^- \to \gamma, Z \to 4$ jets. Defining jets by the Sterman-Weinberg variables ε, δ, one expects that for α_s (92 GeV) = 0.1, σ_{4jet} ($\varepsilon = 0.15$, $\delta = 35^o$) $\simeq$ 4 %. There are some indications from a recent JADE analysis [35] that higher order, i.e. $O(\alpha_s)^3$, corrections to σ_{4jet} may not be small. Thus the cross-section just quoted should be taken as a lower limit. Even with the rather stringent cut-offs indicated here, one expects 4×10^4 $Z^o \to$ 4jet events per 10^6 hadronic decays of the Z^o. Thus, 4 jet rates are not going to be any problem at the Z^o. There are two distributions that have been studied. The first is the distribution in the azimuthal angle, ϕ , defined by Körner, Schierholz and Willrodt [36]

$$\cos\phi = \vec{n}_1 \cdot \vec{n}_2 \qquad (2.20)$$

where the normals $\vec{n}_1$ and $\vec{n}_2$ are defined for the configurations with each hemisphere consisting of two jets

$$n_1 \equiv (\vec{P}_1 \times \vec{P}_2) / |\vec{P}_1||\vec{P}_2|$$
$$n_2 \equiv (\vec{P}_3 \times \vec{P}_4) / |\vec{P}_3||\vec{P}_4| \qquad (2.21)$$

The normalized distributions in ϕ for the oriented (i.e. energy ordered) 2-2 configuration for QCD and "QED" type theories are shown in fig. (6), where results for more relaxed cuts ($\varepsilon = 0.1$, $\delta = 25^o$) are also presented. The QCD curves

show the characteristic enhancement near 180^{o}, where the two lower energetic partons, preferentially the gluons, are close together. The "QED" distribution is rather flat. The statistical significance of the test may be expressed through the average value $\langle\phi\rangle$, given in table 2. With 10^5 hadronic events, the distinction

Table 2. The average value of the KSW azimuthal angle for $e^+e^- \rightarrow$ 4 jet events

Theory \ Cuts	$\varepsilon = 0.1,\ \delta = 25^{o}$	$\varepsilon = 0.15,\ \delta = 35^{o}$
QCD	97.0 ± 0.5^{o}	97.7 ± 0.9^{o}
"QED"	91.5 ± 0.6^{o}	90.3 ± 0.9^{o}

between the two theories amounts to 8σ even with the stringent cut offs.

The other distribution, due to Nachtmann and Reiter [37], aims at studying the different helicity structure of the $G^* \rightarrow GG$ and $G^* \rightarrow Q\bar{Q}$ vertices in fig. (5). The distribution in the variable θ_{31}, defined as the angle between the axis of two almost antiparallel partons of high energy (1 and 2) and of the axis of the other two almost antiparallel partons of lower energies (3 and 4), with the ordering $E_1 > E_2 > E_3 > E_4$ is sensitive to the splitting $G^* \rightarrow GG$ and $G^* \rightarrow Q\bar{Q}$. For reasons of experimental ease, a modified angle, $\bar{\theta}_{31}$, is more appropriate, which is defined as follows

$$\cos\bar{\theta}_{13} = \vec{n}_{12} \cdot \vec{n}_{34} \qquad (2.22)$$

with

$$\vec{n}_{12} = \left(\vec{P}_1/|\vec{P}_1| - \vec{P}_2/|\vec{P}_2| \right)$$

$$\vec{n}_{34} = \left(\vec{P}_3/|\vec{P}_3| - \vec{P}_4/|\vec{P}_4| \right) \qquad (2.23)$$

There were two additional cuts introduced on the 4-jet event sample, namely by requiring $E_3/E_2 < 1/2$ and $\cos\theta_{34} < -0.7$. These cuts reduce the 4-jet sample enormously, leaving only about 6 % of all 4 jet events generated with the indicated (ε, δ) values. The normalized distributions $d\sigma/d|\cos\bar{\theta}_{13}|$ for QCD and "QED" type theories are shown in fig. (7), for the (ε, δ) values indicated. The two distributions are distinguishable. Again, the significance of the test can be indicated through the average value $\langle|\cos\bar{\theta}_{13}|\rangle$, given in table 3.

Table 3. The average value of the modified NR variable defined in (2.22) for $e^+e^- \rightarrow$ 4jet events

Theory \ Cuts	$\varepsilon = 0.1,\ \delta = 25^{o}$	$\varepsilon = 0.15,\ \delta = 35^{o}$
QCD	0.627 ± 0.007	0.483 ± 0.014
"QED"	0.545 ± 0.008	0.445 ± 0.012

The statistical significance of this test is comparable to that of the KSW method. For estimates of background from the fragmentation processes, as well as from the decay $Z^{o} \rightarrow t\bar{t} \rightarrow$ jets we refer to the detailed report by Rudolph in Physics at LEP [19]. Perhaps, it should be remarked here that the stability of these distributions in $O(\alpha_s)^3$ still remains to be tested. These corrections may not turn out to be small!

Next, we discuss the tests of the non-abelian nature in orthotoponium decays $\theta \rightarrow$ 4jets, and $\theta \rightarrow \gamma +$ 3jets. Since, as the top quark mass increases the single

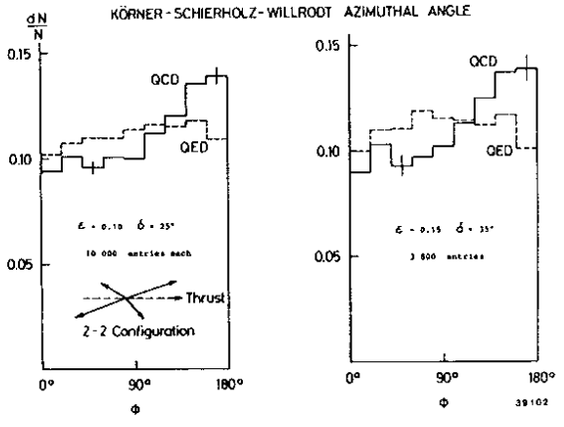

Fig. 6. Normalized distributions in the Körner-Schierholz-Willrodt azimuthal angle, ϕ , for the QCD and "QED" type theories (from ref. (19))

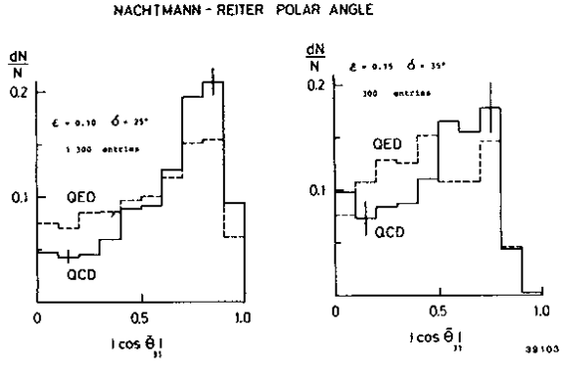

Fig. 7. Normalized distributions in the modified Nachtmann-Reiter variable $|\cos\bar{\theta}_{31}|$ for QCD and "QED" type theories (from (ref. 19))

quark decays of the top quark in θ (= $t\bar{t}$) become dominant, the branching ratios for the QCD processes $\theta \to$ 3jets, 4jets etc. decrease. In addition, since the ratio R for 60 GeV$< \sqrt{s} <$100 GeV (expected value of m_θ) is rather large, there would be copious production of 3 and 4jet events from the non-resonating background $e^+e^- \to \gamma, Z \to$ 3jets, 4jets. The rather large value of m_θ has introduced some non-trivial complications in carrying out the simple QCD tests suggested for the $\theta \to$ 3jets, 4jets final state. This problem deserves further theoretical study. If, however, it turns out that $m_\theta \simeq m_Z$, then since $\Gamma(Z) >> \Gamma(\theta)$, the processes $e^+e^- \to \gamma, Z \to$ 3 jets, 4jets will be dominated by the decays $Z^0 \to$ 3jets, 4jets and the tests that we have just described also hold for this situation. Because of this reason we have concentrated on the radiative decays $\theta \to \gamma +$ 3jets. In discussing these radiative decays, it is instructive to look at the Altarelli-Parisi splitting formula (38)

$$D_{G \to GG}(z,\chi) = 6/2\pi \left\{ (1-z+z^2)^2/(z(1-z)) + z(1-z)\cos 2\chi \right\} \qquad (2.24)$$

$$D_{G \to q\bar{q}}(z,\chi) = n_f/2\pi \left\{ 1/2\left[z^2+(1-z)^2 \right] - z(1-z)\cos 2\chi \right\}$$

with n_f being the number of quark flavour, Z is the momentum fraction of the outgoing parton and χ is the angle of (GG) or ($q\bar{q}$) plane with the linear polarization of the splitting gluon. One expects the dominance of the γGGG final state over $\gamma Gq\bar{q}$, since D(G $\to$ GG) is more singular than D(G $\to q\bar{q}$) near $z \simeq 0$. Since the virtual gluon in $\theta \to \gamma GG^* \to$ GG or $q\bar{q}$ is partly polarized perpendicular to the γ GG* plane, one also expects from the sign of this term in (2.24) that the GG plane tends to be perpendicular to the γ G plane whereas $q\bar{q}$ lies in the same plane. The most suitable angle to study this asymmetry in $\gamma +$ 3jet events

is the angle χ, between the normal to the plane given by the photon and the fastest jet in the hadronic rest frame and the normal to the plane of the other two jets. It turns out that there are clear differences between QCD and the "QED" (= γ Gq$\bar{q}$) events as shown in fig. 8 despite influence of the invariant mass cuts to define the jets.

An interesting distribution involves the polar angle, between the beam axis and the photon. This is shown in fig. (9) where one can see the dependence

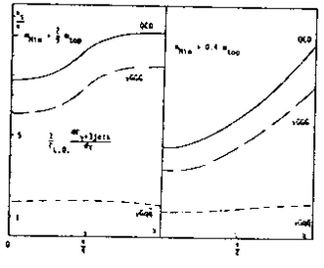

Fig. 8. The azimuthal angle distribution $1/\Gamma_0 \; d\Gamma(\gamma+3jets)/d\chi$ for two m_{min} values
a) $m_{min} \gtrsim 2/9 \; m_{top}$
b) $m_{min} \gtrsim 0.4 \; m_{top}$
Γ_0 is the decay width for $\theta \to \gamma GG$ with the same m_{min} cut-offs
(from Streng in ref. 19)

of the quantity α defined as $d\Gamma/d\cos\theta \sim 1 + \alpha \cos^2\theta$ as a function of m_{min} (minimum invariant mass/m_θ per event). In an abelian (= γ Gq$\bar{q}$) theory one expects a strong decrease of α at large m_{min} contrary to QCD. The problem in this test is probably the rate since the branching ratio for $\theta \to \gamma$ + 3jet is

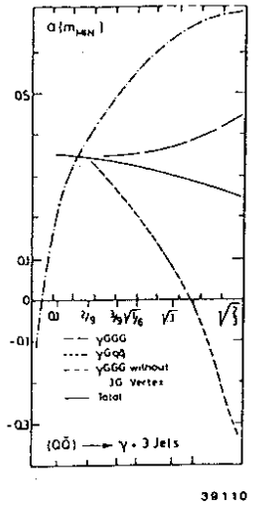

Fig. 9. Average value of the photon polar angle coefficient α for jets as a function of m_{min} (from ref. 19)

not expected to be larger than 1 % for $m_\theta > 80$ GeV. A detailed calculation for the rates assuming various m_{min} cut-offs can be seen in the report by Streng (19) in Physics at LEP.

3. Heavy quark physics at LEP

We shall discuss some selected aspects of heavy quark physics in this section and concentrate on the top and bottom quarks. The present evidence of top quark is rather fragile. As indicated earlier, an interpretation of the lepton-jet-jet

$\not{p}_T$ events in the UA1 detector [39] indicates the presence of a top quark with mass in the range 30-50 GeV. If the UA1 interpretation of this class of events is right, then it should be possible to produce top quarks and measure their decay characteristics at LEP-I and SLC. We have already discussed the $t\bar{t}$ production cross-sections and branching ratios in the decays $Z^0 \to t\bar{t}$. The first order of business at LEP is to determine m_t. We describe the methods already advocated for this purpose, backed up by some more detailed calculations [40].

3.1 Top-quark mass determination

The sensitivity of the branching ratio $BR(Z^0 \to t\bar{t})$ on m_t has already been shown in fig. (3). To make use of this information one should figure out a dependable method to experimentally separate the top quark events. Since the final states in the process $Z^0 \to t\bar{t}$ are expected to be very spherical, as for example shown in fig. (10) for m_t = 35 GeV, a judicious cut on the sphericity variable,

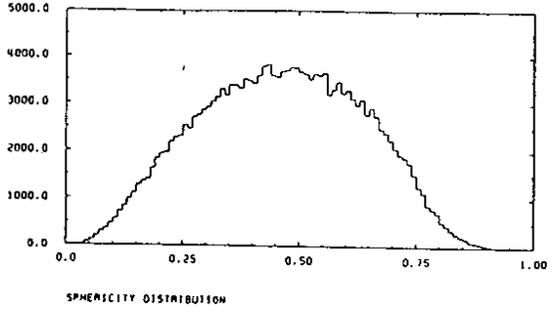

Fig. 10. Sphericity distribution from the process $e^+e^- \to \gamma, Z \to t\bar{t}$ $\longrightarrow$ (hadrons + leptons) at $\sqrt{s}$ = 93 GeV and m_t = 35 GeV (from ref. 40)

S, will still retain a very large fraction of top events, while removing most

of the background. Thus, the cross-section above S = 0.15 (say) is expected to be dominated by the top quarks. Detailed estimates using this method yield an error on m_t of $\sim$ 1.5 GeV for $m_t \sim$ 40 GeV [26].

In order to get much better precision on m_t, the use of inclusive lepton (e,μ,τ) spectra is generally advocated. In the rest frame of the top quark, the lepton energy spectrum from the decay $t \to q\ell^+\nu_\ell$ is given by [41]

$$1/\Gamma \; d\Gamma/dx_\ell = 12 \; \frac{x_\ell^2 (1 - x_\ell - \varepsilon^2)^2}{(1 - x_\ell)} \qquad (3.1)$$

where

$$\varepsilon = m_q/m_t \;, \quad x_\ell = 2E_\ell/m_t$$

Leading order QCD corrections to $d\Gamma/dx_\ell$ were found to be negligible for the normalized x_ℓ distributions [42]. So, it is quite reasonable to continue using (3.1). The shape of the lepton spectrum determines the quark mass ratio ε and hence m_t. There is a slight complication in using this method. At Z^0, top quarks will very likely not be produced at rest; their decay products cannot be well separated and thus their direction not well determined. However, assuming an isotropic angular distribution of the lepton in the rest frame, the energy distribution in the Z^0 rest frame can be generated. A global fit of $d\sigma/dx_\ell$ can then determine m_t. To quantify this well discussed method, we present a slight variation on this general theme. Instead of trying to determine the end-point spectrum, which demands formidable lepton energy resolution, one could measure the integrated lepton spectrum above and below some x_ℓ cut-off. Defining the ratio,

$$R_t(x_c) \equiv \frac{\int_{(x_\ell > x_c)} d\sigma/dx_\ell \,(e^+e^- \to \gamma, Z \to t\bar{t} \to \ell^\pm x)\,dx_\ell}{\int_{(x_\ell < x_c)} d\sigma/dx_\ell \,(e^+e^- \to \gamma, Z \to t\bar{t} \to \ell^\pm x)\,dx_\ell} \qquad (3.2)$$

we show in fig. (11) the ratio $R_t(x_c = 0.5)$ as a function of m_t. The errors shown

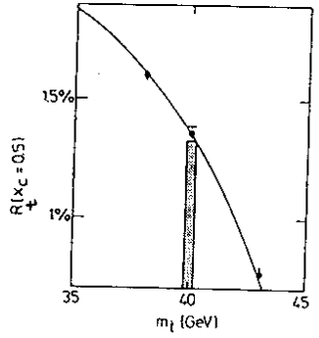

Fig. 11. The ratio $R_t(x_c = 0.5)$ as defined in eq. (3.2) as a function of the top quark mass (from ref. 40)

are statistical, based on a detailed simulation of the $e^+e^- \to t\bar{t} \to \ell^\pm x$ events assuming 100 K $t\bar{t}$ events, which is a typical number expected in Z^0 decays at LEP, with one year of running and m_t around 40 GeV. As can be seen in fig. (11), this method gives an accuracy on m_t of O(200 MeV). It would be difficult to do better than this due to the non-perturbative effects, which certainly are not entirely negligible.

Other methods for top mass determination have also been proposed [26], involving non-leptonic weak decays of the top quarks and determining the invariant mass of the multi-jet system, giving Δm_t sensitivity comparable to the lepton energy method we just discussed. We remark that the fragmentation model dependence may turn out to be the limiting constraint here. These methods are geared for searches of the top quark in Z^0 decays. In the continuum, one would be able to see the top threshold quite precisely. The large contribution of the so-called "Single Quark Decay, SQD" mechanism would force also toponia states to decay weakly. Thus, searches involving energetic $\ell^\pm$ can be used also on $t\bar{t}$ resonances. This method is discussed in detail elsewhere [26].

3.2 Determination of the matrix elements V_{ti}

Apart from the determination of m_t and the "Michel parameter" for the top quark, ρ_t, which determines the chirality of the top quark charged weak current, there are a number of important measurements that have to be done to determine the top quark properties. We recall that the hadronic charged weak currents are governed by the (3x3) flavour mixing CKM matrix. This matrix allows three charged current transitions for the top quark decays, namely

$$\begin{aligned} t &\to bW^+ \\ t &\to dW^+ \\ t &\to sW^+ \end{aligned} \qquad (3.3)$$

where the W^+ is real or virtual depending on m_t.

The branching ratios are determined by the CKM matrix elements $|V_{tb}|^2$, $|V_{ts}|^2$ and $|V_{td}|^2$ for the three transitions shown in (3.3). A quantitative test

of the CKM model lies in checking that the magnitudes of these matrix elements are in agreement with the unitarity bounds obtained from the present experimental information on weak decays. To amplify this point, we use the convenient parameters of the CKM matrix due to Wolfenstein [43]. Writing the CKM matrix symbolically, one has the following representation,

$$V_{CKM} = \begin{pmatrix} V_{ud} & V_{us} & V_{ub} \\ V_{cd} & V_{cs} & V_{cb} \\ V_{td} & V_{ts} & V_{tb} \end{pmatrix}$$

$$\simeq \begin{pmatrix} 1-\frac{1}{2}\lambda^2 & \lambda & A\lambda^3(\rho-i\eta) \\ -\lambda & 1-\frac{1}{2}\lambda^2 & A\lambda^2 \\ A\lambda^3(1-\rho-i\eta) & -A\lambda^2 & 1 \end{pmatrix} \qquad (3.4)$$

The present experimental information on weak decays gives (using $\bar{R} \equiv \Gamma(b\to u\ell\nu_\ell)/\Gamma(b\to c\ell\nu_\ell) < 0.08$)

$$\lambda \simeq 0.23$$
$$A = 1.0 \pm 0.2 \qquad (3.5)$$
$$\rho^2+\eta^2 < 0.65$$

Thus, it is expected that in the three generation model the three matrix elements needed for the transitions (3.3) have the relative magnitudes

$$|V_{tb}| : |V_{ts}| : |V_{td}| \simeq 1 : \lambda^2 : \lambda^3 \qquad (3.6)$$

This would then lead to the branching ratios shown in table (4). Based on this calculation the inclusive rates for the three $t \to q$ transitions are estimated to be

Table 4. Reduced widths, $\bar{\Gamma}_i$, for the top quark decays defined as $\Gamma_i = \frac{G_F^2 m_t^5}{192\pi^3}\bar{\Gamma}_i$. Estimates of branching ratios for $V_{ts} = 0.05$ and $V_{td} = 0.01$ are also shown (from ref. 13)

Modes	Widths $\bar{\Gamma}_i$		BR (%)
$t \to b e \nu_e$	0.79	V_{bt}^2	10.7
$b \mu \nu_\mu$	0.79	V_{bt}^2	10.7
$b \tau \nu_\tau$	0.77	V_{bt}^2	10.5
$b u \bar{d}$	2.38	V_{bt}^2	32.4
$b u \bar{s}$	0.13	V_{bt}^2	1.7
$b c \bar{s}$	2.34	V_{bt}^2	31.9
$b c \bar{d}$	0.12	V_{bt}^2	1.7
$b \bar{b} c$	2.16	$V_{bt}^2 \; V_{bc}^2$	7.5×10^{-2}
$s e \nu_e$	0.87	V_{ts}^2	3×10^{-2}
$s \mu \nu_\mu$	0.87	V_{ts}^2	3×10^{-2}
$s \tau \nu_\tau$	0.86	V_{ts}^2	2.9×10^{-2}
$s u \bar{d}$	2.68	V_{ts}^2	9.1×10^{-2}
$s u \bar{s}$	0.14	V_{ts}^2	4.8×10^{-3}
$s c \bar{s}$	2.44	V_{ts}^2	9.0×10^{-2}
$s c \bar{d}$	0.13	V_{ts}^2	4.7×10^{-3}
$d X$	8.3	V_{td}^2	1×10^{-2}

$$BR(t \to bx) \simeq 1$$
$$BR(t \to sx) \simeq O(10^{-3}) \qquad (3.7)$$
$$BR(t \to dx) \simeq O(10^{-4})$$

The inclusive rates for the two suppressed transitions $t \to sx$ and $t \to dx$ are indeed very small. There are two ways to experimentally distinguish between the three transitions in eq. (3.3). The first method lies in measuring the end point (or the very energetic tail) of the lepton energy spectrum in the semileptonic decays $t \to \ell^+ x$. This would require lepton energy resolutions better than O(100 MeV) for $E_\ell \simeq \mathcal{O}$(20 GeV), which may or may not be available. The other method lies in measuring the inclusive semileptonic decays $t \to (d,s)\, \ell^+ \nu_\ell$, hoping that the (d,s) quarks in the decay would lead to low hadron multiplicity. The decay patterns of charm and bottom quarks seem to have this feature [44].

The event topology for the process

$$Z^0 \to t\,\bar{t}, \quad t \to 3 \text{ jets}, \quad \bar{t} \to (d,s)\, \ell^+ \nu_\ell \qquad (3.8)$$

with the leptonic side jet rather slim would be striking, leading to a "fat-slim" hadronic configuration. The $\ell^\pm$ distribution can be used to remove the background from other sources. The expected small branching ratios for $t \to (d,s)x$, however, may turn out to be the real obstacle, eventually.

There is an <u>indirect</u> method to determine the matrix elements V_{td} and V_{ts} as recently suggested in ref. (18). This lies in the measurements of the

B_d^0-$\bar{B}_d^0$ and B_s^0-$\bar{B}_s^0$ transitions. To discuss this point in detail, we turn to the production and decays of bottom hadrons at LEP.

3.3 Bottom physics at LEP and SLC

Let us briefly recapitulate the present interest in bottom physics and the extent to which experiments at LEP and SLC are expected to contribute to this field. The b-quark is observed to decay via the charged weak current transition

$$b \to cx \qquad (3.9)$$

The other allowed charged current transition

$$b \to ux \qquad (3.10)$$

has not yet been seen. Concentrating on the semileptonic decay modes, the present experimental situation can be summarized as a bound on the quantity $\bar{R}$, defined earlier. Experiments at CESR and DORIS lead to the bound [5]

$$\bar{R} < 0.08 \qquad (3.11)$$

though we hasten to add that there is considerable uncertainty on this bound due to the bottom hadron wave function effects. The first question in bottom physics at LEP to investigate is the determination of the limit on $\bar{R}$, or for that matter on the ratio $b \to u/b \to c$, which is obtainable from LEP experiments. It has repeatedly been pointed out that the shapes and end points of $\ell^\pm$ spectra from the decays $b \to \ell^\pm x$ depend on the b quark mass m_b and the mass difference. Thus in the free quark decay model $b \to (c,u)\, \ell^- \nu_\ell$, the maximum lepton energy is given by $\frac{m_b^2 - m_c^2}{2m_b}$ and $\frac{m_b^2 - m_u^2}{2m_b}$ for the $b \to c$ and $b \to u$ transitions, respectively. This difference has already been exploited to put a bound on $\bar{R}$ from the lepton energy spectra in the process $e^+e^- \to \Upsilon(4s) \to B\bar{B} \to \ell^\pm x$. As shown in ref. (13), the interesting distribution at LEP in this context is the lepton

transverse-momentum distribution, $1/N\ dN/dp_T^l$. The p_T^l spectra, measured with respect to the bottom quark axis, were calculated in ref. (41) on the assumption of free quark decay model. These distributions, which are stable with respect to the $O(\alpha_s)$ QCD corrections, are shown in fig. 12. Systematic errors due to p_T broadening, jet-axis determination and typical energy resolutions give reasons

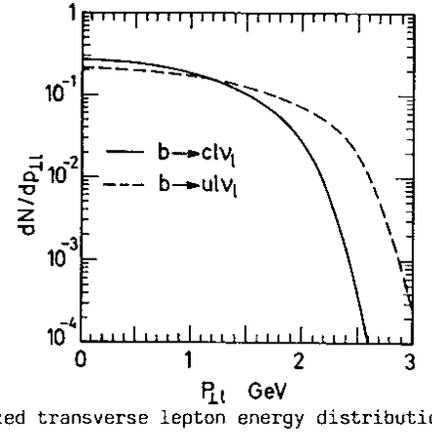

Fig. 12. The normalized transverse lepton energy distribution $1/N\ dN/dp_T^l$ for the decays $b \to u\, l^+ \nu_l$ and $b \to c\, l^+ \nu_l$ (from ref. 13)

to be confident about the workability of this method. We remark that a measurement of $\bar{R}$ at and above $\bar{R} = 0.01$ will be feasible at LEP experiments. The determination of V_{bu} from $\bar{R}$ is subject to some theoretical uncertainty as is by now well appreciated. Our emphasis here on the measurement of the ratio $\bar{R}$ is not random; at LEP it may turn out to be the only method for a reliable measurement of the CKM matrix element V_{bu}. We remark that a knowledge of $\bar{R}$ provides very tight constraints on the internal consistency of the standard model. To illustrate this point, we show in fig. 13 the constraints on the top quark mass m_t, provided by the measurements of the bottom lifetime, τ_B, the CP-violation parameter in the kaon system, ε_K, and the upper bound $\bar{R} = 0.05$. Though the standard model is consistent at present with data, as shown in fig. 13 for the assumed value

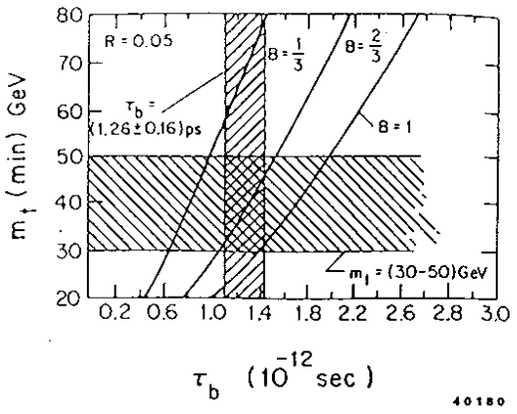

Fig. 13. The minimum value of the top quark mass, m_t, compatible with ε_K in the standard model for $\bar{R} = \Gamma(b \to u\, e\, \nu_e)/\Gamma(b \to c\, e\, \nu_e) = 0.05$ as a function of the bottom lifetime, τ_b, for three values of the bag constant B = 1/3, 2/3 and 1 (from Buras, Slominsky and Steger in ref. 46). The constraints become more stringent for smaller values of $\bar{R}$.

of $\bar{R}$, a value significantly below 0.05 will only be consistent with ε_K and τ_B measurements if m_t is very large [45]. Since m_t will, in all likelihood, be measured at LEP, the standard model will be faced with a very stringent test. In fact, determination of $\bar{B}$ and m_t provides the first non-trivial test to check if CP violation is indeed described by the standard CKM model.

Continuing the discussion of the bottom quark properties and their determination in LEP experiments, there are two important issues in addition that we would like to focus on. The first issue concerns the measurements of the strength of the so-called $|\Delta B| = 2$, $\Delta Q = 0$ transitions leading to B_d^0-$\bar{B}_d^0$ and B_s^0-$\bar{B}_s^0$ oscillations. The other issue is related to the possibility of measuring CP violation in the bottom sector.

In discussing the B-$\bar{B}$ oscillations we recall that there are two neutral bottom mesons $B_d^0 = (b\bar{d})$ and $B_s^0 (= b\bar{s})$ which could mix with their charge conjugates $\bar{B}_d^0$ and $\bar{B}_s^0$, respectively. The box diagrams responsible for the mass difference $\Delta M(B_d^0)$ and $\Delta M(B_s^0)$ are shown in fig. 14. These diagrams give rise to the following contributions

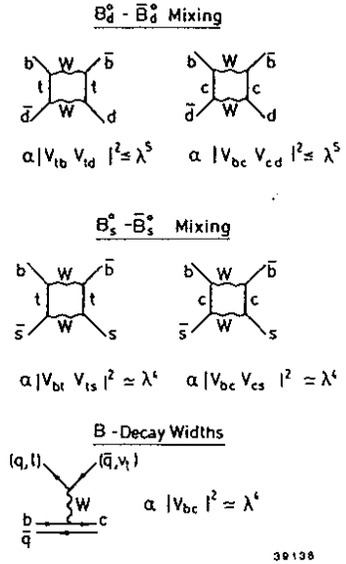

Fig. 14. Standard model contributions to the mass difference $\Delta M(B_d^0)$ and $\Delta M(B_s^0)$ for the two neutral bottom meson systems B_d^0-$\bar{B}_d^0$ and B_s^0-$\bar{B}_s^0$. The dominant contribution to the (common) bottom hadron decay widths is also shown. For each diagram, the CKM angle dependence is also shown in terms of $\lambda = \sin\theta_c$.

$$x_d \equiv \frac{\Delta M(B_d^0)}{\Gamma_d} = \frac{G_F^2 f_{Bd}^2 m_{Bd}}{6\pi^2 \Gamma_d} m_W^2 \mathcal{B} F_d(m_b, m_t, \lambda)$$

$$x_s \equiv \frac{\Delta M(B_s^0)}{\Gamma_s} = \frac{G_F^2 f_{Bs}^2 m_{Bs}}{6\pi^2 \Gamma_s} m_W^2 \mathcal{B} F_s(m_b, m_t, \lambda) \qquad (3.12)$$

where f_{B_d} (f_{B_s}) is the B_d^0 (B_s^0) pseudoscalar meson coupling constant and $\mathcal{B}$ is the so-called bag constant, expected to be close to 1 for bottom hadrons. The function $F_{d,s}(m_b, m_t, \lambda)$ depends on quark masses and the CKM matrix elements and are dominated by the top quark contribution.

$$F_d(m_b, m_t, \lambda) = \mathcal{U}_t |\lambda_{td}|^2$$
$$F_s(m_b, m_t, \lambda) = \mathcal{U}_t |\lambda_{ts}|^2 \qquad (3.13)$$

To a very good approximation the quark mass functions $\mathcal{U}_t$ can be expressed as (46)

$$\mathcal{U}_t = m_t^2/m_W^2 \, \eta^B + \mathcal{O}(m_b^2/m_t^2) \qquad (3.14)$$

where η^B is a QCD correction factor estimated to lie in the range $0.81 \leq \eta^B \leq 0.86$, for 25 GeV $\leq m_t \leq$ 60 GeV and 0.1 GeV $< \Lambda_{\overline{MS}} <$ 0.2. The CKM factors λ_{td}, λ_{ts} in eqs. (3.13) are given by

$$|\lambda_{td}| = |V_{tb}^* V_{td}| \simeq |V_{td}|$$
$$|\lambda_{ts}| = |V_{tb}^* V_{ts}| \simeq |V_{ts}| \qquad (3.15)$$

It is clear from eqs. (3.12)-(3.15) that once m_t is known, measurements of the mixing ratios x_d and x_s are equivalent essentially to measuring the CKM matrix elements V_{td} and V_{ts}, respectively, as we had indicated earlier in the discussion of the top quark physics. To get estimates of x_d and x_s, we put in the measured life-time $\tau_b = (1.11 \pm 0.14) \times 10^{-12}$ sec, which gives $\Gamma_d = \Gamma_s = (5.93^{+0.86}_{-0.66}) \times 10^{-13}$ GeV and use currently popular values for Bf_{B_d} and Bf_{B_s},

which have been obtained using QCD sum rules [47]

$$Bf^2_{B_d} = (0.11\ \text{GeV})^2$$
$$Bf^2_{B_s} = (0.15\ \text{GeV})^2 \qquad (3.16)$$

These numbers give [18]

$$x_d = 0.05\,(m_t/40\,\text{GeV})^2\,(Bf^2_{Bd}/(110\,\text{MeV})^2)\,(\lambda_{td}/\lambda^3)^2$$
$$x_s = 1.75\,(m_t/40\,\text{GeV})^2\,(Bf^2_{Bs}/(150\,\text{MeV})^2)\,(\lambda_{ts}/\lambda^2)^2 \qquad (3.17)$$

where we have made all the relevant dependences in x_d and x_s explicit. The normalization of λ_{td} and λ_{ts} above in terms of the parameter λ has been motivated by the Wolfenstein parametrization, as indicated in eq. (3.5). The measures x_d and x_s are plotted as functions of m_t in fig. 15 with the preferred values of the coupling constants and mixing angles as indicated in eqs. (3.16) and (3.17). Thus, one expects significant, perhaps complete mixing corresponding to $x_s \gg 1$, for the B^0_s-$\bar{B}^0_s$ sector and small mixing in the B^0_d-$\bar{B}^0_d$ sector, with $x_d < 0.1$, a reasonable upper bound in the standard model.

We shall now discuss the phenomenology of B^0-$\bar{B}^0$ mixings. Since the lifetime of the bottom hadron is very short to enable time dependent measurements, as opposed to the case in the K_L-K_S regeneration, only time integrated

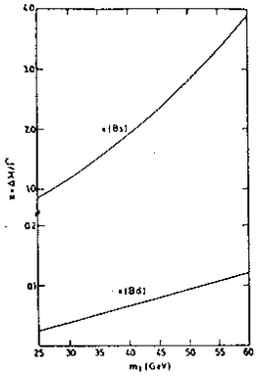

Fig. 15. Estimates of the mixing quantities $x(B_s) = \Delta M/\Gamma(B^0_s)$ and $x(B_d) = \Delta M/\Gamma(B^0_d)$ in the standard model for B^0_s-$\bar{B}^0_s$ and B^0_d-$\bar{B}^0_d$ mixings, respectively, as a function of the top quark mass, m_t (from ref. 13)

effects of B^0-$\bar{B}^0$ mixing are measurable at LEP. A useful measure for this purpose was introduced in ref. (48), namely the ratio of "wrong-sign" to "right-sign" lepton in the semileptonic decays of M^0 and $\bar{M}^0$. Adhering to the convention of the particle data group [49], the "right sign" lepton in bottom hadron decays is

$$B_q \to \ell^+ X \qquad (3.18)$$

the "wrong-sign" lepton is then

$$B_q \to \ell^- X \qquad (3.19)$$

A time-integrated measure of B^0-$\bar{B}^0$ mixing is then defined as follows (Γ is the partial width)

$$r_q = \frac{\Gamma(B^0_q \to \ell^- X)}{\Gamma(B^0_q \to \ell^+ X)}, \qquad q = d, s \qquad (3.20)$$

one can then easily show that the mixing probability r_q is simply related to x_q and y_q ($y_q \equiv (\Delta\Gamma/2\Gamma)_q$ with $\Gamma_q = (\Gamma_H + \Gamma_L)_q/2$) by

$$\begin{aligned} r_q &= (x_q^2 + y_q^2)/(2 + x_q^2 - y_q^2) \\ &\simeq x_q^2/(2+x_q^2) \\ &\longrightarrow 1 \\ &\quad x_q \gg 1 \end{aligned} \tag{3.21}$$

The life-time difference dependent quantities y_d, y_s are very small compared to x_d and x_s and can be neglected in the estimates of r_q. In the standard model one expects [13]

$$\begin{aligned} r_d &\leqslant 10^{-2} \\ r_s &= 0.3 - 1 \end{aligned} \tag{3.22}$$

which can easily be obtained by using eq. (3.21) and the functions x_d, x_s given in fig. 15. It is important to point out that the nomenclature "wrong-sign leptons" and "right-sign leptons" used above in defining eqs. (3.18), (3.19) applies only to the primary decays of the b quark givign $b \to \ell^- x$. Thus, it is important to suppress the secondary leptons from the cascade $\bar{b} \to \bar{c}x \to \ell^- x$ etc. For experimental analyses it is often found useful to define a variable χ

$$\chi \equiv \Gamma(B \to \ell^- X)/\Gamma(B \to \ell^{\pm} X) \tag{3.23}$$

The variable χ, which is an average over the bottom mesons produced in a given

experiment, is related to the ratios χ_q, specific to the bottom hadrons B_d^0 and B_s^0 by the relation

$$\begin{aligned} \chi &= \left[(BR)_d P_d \chi_d + (BR)_s P_s \chi_s \right]/\langle BR \rangle \\ &\simeq P_d \chi_d + P_s \chi_s \end{aligned} \tag{3.24}$$

where P_d and P_s are, respectively, the probability that a b quark produced in a high energy collision will end up in a $\bar{B}_d^0$ (= $b\bar{d}$) or $\bar{B}_s^0$ (= $b\bar{s}$) meson. The quantities $(BR)_d$, $(BR)_s$ and $\langle BR \rangle$ are the semileptonic branching ratios of the B_d^0, B_s^0 mesons and the average over bottom hadrons, respectively. One expects them to be approximately equal. Using the values [50]

$$\begin{aligned} P_d &= 0.35 - 0.40 \\ P_s &= 0.15 - 0.20 \\ \chi_d &= 10^{-2} \\ \chi_s &= 0.5 \end{aligned} \tag{3.25}$$

one expects $\chi = 0.08 - 0.1$ in the standard model.

Turning to the actual measurement of the B^0-$\bar{B}^0$ mixing effects, we recall that there are three different methods proposed to measure them, which are described below.

(i) Same-sign dilepton production

The process of interest is

$$e^+e^- \to \gamma, Z \to b\bar{b}x \to \ell^{\pm}\ell^{\pm}x, \ell^+\ell^-x \qquad \ell = e, \mu, \tau \tag{3.26}$$

Concentrating on the leptons from the primary b decays $b \to \ell^- x$ and defining N^{+-} (N^{++}) the total number of opposite sign (same sign) dileptons produced in a reaction like (3.26), one can show that the ratio $R(^{++}/_{--}/+-)$ defined below, obeys the relation

$$R(^{++}/_{--}/+-) \equiv (N^{++} + N^{--})/N^{+-} = 2\chi(1-\chi)/[\chi^2 + (1-\chi)^2] \qquad (3.27)$$

For χ in the range 0.05 - 0.1, as expected in the standard model, the ratio $R(^{++}/_{--}/+-)$ lies in the range 0.1 - 0.22. We remark that all non-bottom primary leptons have been removed from N^{++}_{--}, N^{+-}, entering eq. (3.27). The present experimental bounds on the quantity χ in e^+e^- annihilation are as follows:

$$\chi(e^+e^-, \sqrt{s} = 29\,GeV) < 0.12 \qquad \text{(90 \% C.L.) MARK II [51]}$$

$$\chi_d(e^+e^-, \Upsilon(4S)) < 0.11 \qquad \text{(90 \% C.L.) ARGUS [52]} \qquad (3.28)$$

On the other hand experimental search in $\bar{p}p$ collisions at the CERN sp$\bar{p}$s have lead to positive results. The UA1 collaboration [53] has measured the ratio in question, giving

$$R(^{++}/_{--}/+-)_{UA1} = 0.46 \pm 0.07 \pm 0.03 \qquad (3.29)$$

The estimates of the background are [18]

$$R(^{++}/_{--}/+-)_{Bgd.} = 0.24 \pm 0.05 \qquad (3.30)$$

reflecting the uncertainties due to the poor determination of m_t and fragmentation/decay properties of the charm and bottom quarks. Interpreting the mismatch between (3.27) and (3.28) in terms of B^0-$\bar{B}^0$ mixing, one gets [18],

$$\chi(p\bar{p}, \sqrt{s} = 630\,GeV) = 0.125 \pm 0.05 \qquad (3.31)$$

which is, within errors, compatible with negative results in e^+e^- annihilation (MARK-II result), and with the ARGUS limit $\chi_d < 0.11$, only if mixing is substantial in the B_s^0-$\bar{B}_s^0$ sector. The result of the present data analysis and the expected values of the mixing probabilities are shown in fig. (16). At 68 %

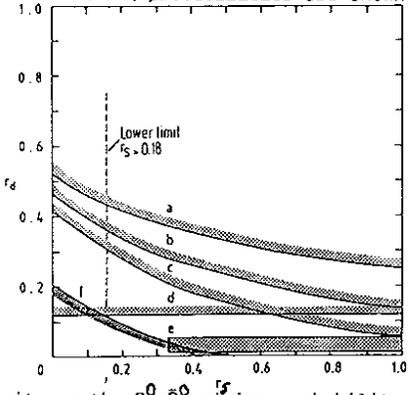

Fig. 16. Upper limits on the B_d^0-$\bar{B}_d^0$ mixing probability, r_d, and the B_s^0-$\bar{B}_s^0$ mixing probability, r_s, from e^+e^- experiments (curves a-d), the standard model prediction (curve e) and the lower limits on r_d and r_s from the UA1 dimuon ratio $R(^{++}/_{--}/+-)$ (curve f) (from ref. 53).
(a)-(c) MARK II limits (51) with (a) $P_d = 0.35$ $P_s = 0.10$,
(b) $P_d = 0.375$, $P_s = 0.15$, (c) $P_d = 0.4$, $P_s = 0.2$, (d) ARGUS limits from $\Upsilon(4s) \to B\bar{B}$ (52), (e) Standard Model estimates (13)
(f) UA1 limits with $P_d = 0.4$, $P_s = 0.2$

C.L., the data gives a lower limit on χ_s, namely $P_s \chi_s > 0.03$, which for

P_s = 0.20 gives $\chi_s > 0.18$.

If, however, one interprets the UA1 measurement (3.31) in the context of the standard model, then one could obtain a 2σ lower bound on χ_s (or χ_s). This is obtained by setting χ_d = 0 (standard model expectation give $\chi_d \simeq 0(10^{-2})$). The resulting lower bound on χ now gives

$$P_s \chi_s > 0.025$$

which for P_s = 0.20 gives $\chi_s > 0.14$(at 2σ). In fig. 17 are shown the bounds

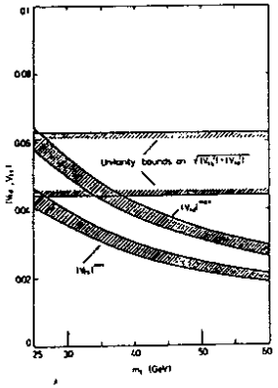

Fig. 17. Upper bound on the CKM matrix element $|V_{td}|$ and the lower bound on $|V_{ts}|$ from the limits $\chi_d < 0.12$ (ARGUS) and $\chi_s > 0.14$ (UA1) as a function of the top quark mass, m_t. The bounds for $|V_{td}|^{max.}$ and $|V_{ts}|^{min.}$ correspond to the $\pm 1\sigma$ allowed values of the bottom lifetime, $\tau_B = (1.11 \pm 0.14) \times 10^{-12}$ sec. The (m_t independent) unitarity bounds on $(V_{td}^2 + V_{ts}^2)^{1/2}$ in the standard model are also shown (from ref. 18)

on the CKM matrix elements $|V_{td}|^{max}$ and $|V_{ts}|^{min}$ as functions of m_t from the limits on χ_d and χ_s

$$\chi_d < 0.12 \qquad \text{(ARGUS)}$$

$$\chi_s > 0.14 \qquad \text{(UA1+SM)}$$

This bound gives (for m_t = 40 GeV)

$$|V_{td}| < 0.042$$
$$|V_{ts}| > 0.030$$

These bounds are consistent with the bounds on $V_{td}^2 + V_{ts}^2$ obtained from unitarity in the standard three-family model, as can be seen in fig. 17. However, a determination of m_t and precise measurements of χ_s will certainly provide a very stringent test of the standard model.

It is extremely important to check the UA1 result (3.27) by independent measurements. Experiments at LEP are obvious places to perform such measurements. We remark that data taken at Υ(4s) are sensitive only to χ_d, for which the standard model expectations are very tiny, $\chi_d \sim 0.01$, and the experiments in e^+e^- continuum at PETRA and PEP presently lack the required statistics. With $O(10^6)$ bottom hadrons available per year at LEP and having good lepton detection efficiency over a large solid angle, we estimate that it would be possible to measure the quantity χ at the level $\chi \gtrsim 0.03$. Since the expectations in the standard model are higher, namely $\chi \gtrsim 0.05$, we are quite optimistic that experiments at LEP will provide positive results in testing B^0-$\bar{B}^0$ mixing by measuring the ratio $R(^{++}_{--}/_{+-})$.

(ii) Electroweak forward-backward charge asymmetry

In e^+e^- annihilation, the forward-backward charge asymmetry arises due to the (γ- Z) interference. In the case of bottom quark production it is usually measured by the lepton from the decay of bottom quarks, giving rise to the process

$$e^+e^- \rightarrow b\bar{b} \rightarrow \ell^- X \qquad (3.32)$$

Since B^0-$\bar{B}^0$ mixing will flip the sign of the lepton [54] it will reduce the charge asymmetry due to purely electroweak interference effects. Denoting by $(A^b_{FB})_0$ the asymmetry for the no mixing case (i.e. for $\chi = 0$) and by A^b_{FB} the actual experimental measurement, one can show that the ratio a^b_χ, defined below, satisfies the relationship

$$a^b_\chi \equiv A^b_{FB} / (A^b_{FB})_0 = 1 - 2\chi \qquad (3.33)$$

For $\chi \leqslant 0.10$, one expects $a^b_\chi \gtrsim 0.80$.

This method has been used by the JADE collaboration at PETRA [54] to set an upper limit on χ

$$\chi(e^+e^-, \sqrt{s} = 35\ GeV) < 0.13 \ (90\ \%\ C.L.) \qquad (3.34)$$

which is slightly worse than the one obtained by the MARK II collaboration from same-sign dilepton searches.

Quantitative estimates of B^0-$\bar{B}^0$ mixing effects on the bottom quark charge asymmetry for a typical experimental set up at LEP have been obtained. This method can be used in conjunction with the measurements of $R(^{++}_{--}/+-)$ to augment B^0-$\bar{B}^0$ mixing effects.

(iii) Inclusive final states $b \rightarrow \ell^- K^+ K^+ X$

This proposal consists of measuring the "decay" of an excited bottom quark produced in a hard collision, like for example in $e^+e^- \rightarrow b\bar{b}$ at LEP, decaying into the following state [55]

$$"b" \rightarrow \ell^+ K^- K^- X \qquad (3.35)$$

or its charge conjugate "$\bar{b}$" $\rightarrow \ell^- K^+ K^+ X$. Neglecting small contributions from the Cabibbo suppressed processes and removing soft kaons, $K^\pm$, from the sea, one can show that a good test of the B^0_s-$\bar{B}^0_s$ mixing measure, χ_s, is the ratio involving the inclusive states $\ell^+ K^- K^- X$ and $\ell^- K^- K^- X$, which satisfies the relation [55],

$$R(\ell^+K^-K^-/\ell^-K^-K^-) = \chi_s/(1-\chi_s) \times BR(F^- \rightarrow K^- X)/BR(F^+ \rightarrow K^- X) \qquad (3.36)$$

where it is tacitly assumed that the ℓKK are the products of a single quark. Thus, one needs to know the branching ratios for $F^- \rightarrow K^\pm X$ to estimate $R(\ell KK)$, which, hopefully, should become available by the start of LEP experiments. On the other hand, the measure (3.36) provides more information on B^0-$\bar{B}^0$ mixing than the measurement of $R(^{++}_{--}/+-)$ and a^b_χ, in that it is sensitive only to the B^0_s-$\bar{B}^0_s$ mixing. The ratio defined in (3.36) is certainly measurable at LEP and SLC in experiments having good $\ell^\pm$ and $K^\pm$ detection abilities. The dependence

of R(ℓKK) is shown in fig. (18).

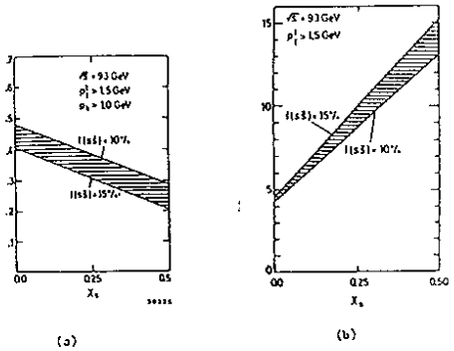

Fig. 18. The ratio (a) R(1KK) and (b) R(11) as function of the mixing measure χ_s with the indicated values of the parameters in e^+e^- annihilation. Here R(11) = (N++ + N--)/(N++ + N-- + N+-) (from ref. 13)

In the rest of this section, we shall briefly entertain the possibility of measuring CP violation in LEP experiments. Concentrating on the dilepton final states in the process (3.26), which we discussed in the context of measuring B^0-$\bar{B}^0$ mixings, we recall that an inclusive measure of CP violation is the "dilepton charge asymmetry", defined as

$$a \equiv (N^{++} - N^{--})/(N^{++} + N^{--}) \simeq 2Z \qquad (3.37)$$

where $Z = 1/2\ \mathrm{Im}\ (\Gamma_{12}/M_{12})$. The counting rates are determined by the total charge asymmetry

$$a^{B\bar{B}}_{total} \equiv (N^{++} - N^{--})/N_{2\ell} = 2a\chi(1-\chi) \qquad (3.38)$$

where $N_{2\ell}$ is the total number of dileptons from the process (3.26). In the standard model one expects [13]

$$a_d^{max} \lesssim 10^{-2}$$
$$a_s^{max} \lesssim 5 \times 10^{-4} \qquad (3.39)$$

with the actual values depending on the CKM matrix element V_{bu} and the phase δ_{KM}, as can be seen in fig. 19. The explicit dependence of the total charge

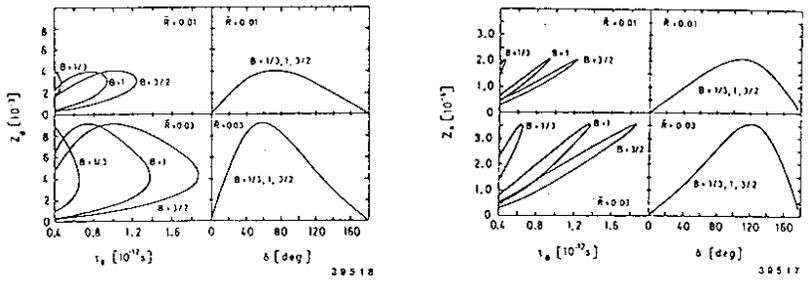

Fig. 19. The CP-violating parameter Z defined as $Z = 1/2\ \mathrm{Im}\,\Gamma_{12} / M_{12}$ for the neutral bottom meson sector with the indicated values of the Bag constant, B, and the ratio $\tilde{R}$ (from Buras et al. in ref. 46)
(a) Z_d for B^0_d-$\bar{B}^0_d$ mixings
(b) Z_s for B^0_s-$\bar{B}^0_s$ mixings

asymmetry, $a^{B\bar{B}}_{total}$, on the quantities specific to B_d-$\bar{B}_d$ and B_s-$\bar{B}_s$ mesons can be expressed as follows [13],

$$a^{B\bar{B}}_{total} = 2a_d\chi_d \frac{(BR)_\ell P_d}{\langle BR\rangle} + 2a_s\chi_s \frac{(BR)_s P_s}{\langle BR\rangle} \qquad (3.40)$$

which on using the values shown in (3.25) gives

$$a^{B\bar{B}}_{total} \lesssim 10^{-4} \qquad (3.41)$$

This means that one would need $\mathcal{O}(10^7)$ bottom hadrons to measure $a^{B\bar{B}}_{total}$ at the level predicted by the standard model! It would take dedicated running of LEP for several years and one will have to combine data from all experiments to get a positive signal in $a^{B\bar{B}}_{total}$. Though the prospects look dim, we certainly think the stakes in CP violation measurements in the bottom sector are high and the details of the estimates on $a^{B\bar{B}}_{total}$ are worth recording. It may, however, turn out that CP violation effects in bottom hadron sector are indeed much larger than the standard model estimates (3.41). Such scenarios exist, for example, in supersymmetric theories [56]. One of the aims of physics at LEP is to measure fine effects and rare processes in the standard model. We emphasize that so little is known about the mechanism of CP violation that the possibility of the inadequacy of the standard model must not only be kept open but also investigated experimentally.

There are other proposals to measure CP violation in bottom decays [57], but since most of these tests involve specific decay modes of bottom hadrons which are difficult to measure at LEP, we don't pursue them here in the context of CP violation searches at LEP.

4. Summary and outlook

We have discussed some salient features of QCD and heavy quark physics at LEP and SLC. Among the former, tests of non-abelian character occupy a special

place. Detailed calculations both in $Z^0 \to$ 4jets and $\theta(t\bar{t}) \to$ 4jets, 3jets + γ decays give reason to be optimistic about the doability of these experiments. The problem of non-perturbative effects should also be under control at LEP energies, because of a factor 2 increase between the highest PETRA energy and m_Z and m_θ, where probably most of the LEP/SLC data will be obtained.

One expects a very rich research programme at LEP and SLC in studies of heavy quark physics. In all likelihood, the $t\bar{t}$ final states should be present in the LEP-I and SLC data. The relative abundance, however, depends on m_t. One should be able to get a rather precise determination of m_t (σ(200 MeV) in LEP experiments as opposed to the present $p\bar{p}$ collider estimates, which have an accuracy on m_t of O(20 GeV). In addition, the V-A character and the canonical decay modes of the top quark should be easy to measure. The problem of measuring the CKM suppressed transitions $t \to (d,s)x$ is, however, very formidable, unless the matrix element V_{tb} turns out to be significantly below 1. This will happen only if there are more than three generations of leptons and quarks, for which there is no motivation for the time being.

The CKM matrix elements V_{td} and V_{ts}, however, can be determined if one measures the mixing probability χ_d and χ_s in the B_d-$\bar{B}_d$ and B_s-$\bar{B}_s$ complex, respectively. We have reviewed the present experimental situation and projections for LEP. Of equally great phenomenological interest is the matrix element V_{bu}, which is, in principle, also measurable in LEP experiment. We estimate that a measurement of V_{bu} should be possible at LEP if the ratio $\bar{R}$ turns out to be bigger than 0.01. In particular, we have discussed at length the non-trivial tests of the standard model that will become available through the measurements of some or all of the parameters, $\bar{R}$, m_t, χ_d, χ_s, and the CP-violating asymmetry $a^{B\bar{B}}_{total}$

Acknowledgements

I would like to thank the organizers of the Winter Meeting at St. Feliu, in particular Tony Mèndez and Merçe Pascual, for a very enjoyable stay. I thank Fernando Barreiro, not only for his help with the Spanish visa and his warm hospitality in Spain but also for many helpful discussions which I have had with him. Finally, I thank Frau Helga Laudien for a patient typing of the manuscript.

References

(1) D.P. Barber et al. (MARK J Collaboration), Phys. Lett. 43, 830 (1979); Ch. Berger et al. (PLUTO Collaboration), Phys. Lett. 86B, 418 (1979); R. Brandelik et al. (TASSO Collaboration), Phys. Lett. 86B, 243 (1979)

(2) For experimental surveys see, for example, F. Barreiro, DESY report DESY 85-008 (1985); S. Bethke, DESY report 86-115 (1986); R.Y. Zhu, Proceedings of the 1984 DPF Conference, Santa Fe, 224 (1984); S.L. Wu, Phys. Rep. 107C, No. 2-5 (1984)

(3) Three different type of non-perturbative models, based on independent fragmentation, the Lund strings and pure phase space, are generally used in the analysis of e^+e^- data at PETRA and PEP, none of which describes the data completely satisfactorily, despite periodic outbursts of euphory on the part of experimental physicists for one or the other of these models.

(4) M.L. Perl, Annu. Rev. Nucl. Part. Sci. 30, 299 (1980)

(5) For a recent review see, for example, M. Gilchrese, proceedings of the XXII International Conference on High Energy Physics, Berkeley, California, USA (1986)

(6) S.L. Glashow, Nucl. Phys. 22, 579 (1961); S. Weinberg, Phys. Rev. Lett. 19 1264 (1967); A. Salam, in Elementary Particle Theory, ed. N. Svartholm (Almquist and Wiksell, Stockholm 1968)

(7) The subject of Higgs searches at LEP is reviewed by H. Baer et al., in Physics at LEP, CERN Report 86-02, vol. 1 (1986)

(8) For a review in e^+e^- annihilation see G. Barbiellini et al., in Physics at LEP, CERN Report 86-02, vol. 2 (1986)

(9) For theoretical surveys see, for example, A. Ali, DESY report 81-016 (1981) and proceedings of the 5th International Summer College, Nathiagali, Pakistan (1981); G. Kramer, DESY report 83-068 (1983); G. Altarelli, Univ. of Rome Preprint 477 (1985)

(10) W. Bartel et al. (JADE Collaboration), Phys. Lett. 115B, 338 (1982); DESY report 86-086 (1986); See also M. Chen, Proceedings of the Ettore Majorana International School of Subnuclear Physics, Erice, Sicily, Italy (1985)

(11) A detailed discussion and references to earlier work can be found in A. Ali et al., in Physics at LEP, CERN report 86-02, vol. 2 (1986)

(12) B.R. Webber, Nucl. Phys. B238, 492 (1984); G. Marchesini, B.R. Webber, Nucl. Phys. B238, 1 (1984)

(13) For a recent review see A. Ali, DESY report 86-041 (1986), and in Physics at LEP, CERN report 86-02, vol. 2 (1986)

(14) N. Cabibbo, Phys. Rev. Lett. 10, 531 (1963); M. Kobayashi and K. Maskawa, Prog. Theor. Phys. 49, 652 (1973)

(15) J. Ellis et al., Nucl. Phys. B131, 285 (1977); A. Ali and Z.Z. Aydin, Nucl. Phys. B148, 165 (1979)

(16) N.G. Deshpande, G. Eilam and A. Soni, Phys. Rev. Lett. 57, 1106 (1986); See also N.G. Deshpande, in Proceedings of the Topical Congference on Supercollider Physics, Eugene, Oregon, U.S.A. (1985)

(17) For recent reviews see A. Ali (in ref. 13); I.I. Bigi and A.I. Sanda, SLAC reports SLAC-PUB-3949 (1986); I.I. Bigi, SLAC-PUB-4001 (1986); Dan-di Wu, Institute of High Energy Physics, Beijing report BIHEP-TH-85-27 (1985)

(18) A. Ali, B. van Eijk and I. ten Have, DESY report 86-108 (1986); CERN report CERN-TH-4523/86 (1986)

(19) G. Rudolph, in Physics at LEP, CERN report 86-02, vol. 2 (1986); K.H. Streng, ibid., vol. 2 (1986)

(20) W.A. Bardeen, A.J. Buras, D.W. Duke and T. Muta, Phys. Rev. D18, 3998 (1978)

(21) M. Dine and J. Sapirstein, Phys. Rev. Lett. 43, 668 (1979); K.G. Chetyrkin, A.L. Kataev and F.V. Tkachov, Phys. Lett. 85B, 277 (1979); W. Celmaster and R.J. Gonsalves, Phys. Rev. Lett. 44, 560 (1980)

(22) H.J. Behrend et al. (CELLO Collaboration), DESY report 86-133 (1986)

(23) J.H. Kühn and P.M. Zerwas, CERN report TH-4089 (1985); F. Gilman and P. Franzini, SLAC PUB 3541 (1985); L.J. Hall, S.F. King and S.R. Sharpe, Harvard Preprint HUTP-85/A012 (1985); F.M. Renard, Zeit. f. Phys. C1, 225 (1979)

(24) J.H. Kühn and S. Ono, Zeit. f. Physik C21, 395 (1984); J. Jersak, E. Laermann and P. Zerwas, Phys. Rev. D25, 1219 (1982); S. Güsken, J.H. Kühn and P.M. Zerwas, Phys. Lett. 155B, 185 (1985)

(25) B.W. Lynn, M.E. Peskin and R.G. Stuart, SLAC-PUB-3725 (1985); W. Hollik and H.-J. Timme, DESY report 85-099 (1985)

(26) For a review and references to earlier work see, W. Buchmüller et al., in Physics at LEP , CERN report 86-02, vol. 1 (1986)

(27) For a recent update on these numbers see, for example, W.J. Marciano, proceedings of the XXIInd International Conference on High Energy Physics, Berkeley, California, USA (1986)

(28) R.F. Schwitters et al., Phys. Rev. Lett. 35, 1320 (1975); G.G. Hanson et al., Phys. Rev. Lett. 35, 1609 (1975)

(29) G. Sterman and S. Weinberg, Phys. Rev. Lett. 39, 1436 (1977)

(30) C.L. Basham, L.S. Brown, S.D. Ellis, S.T. Love, Phys. Rev. D17, 2298 (1978), Phys. Rev. Lett. 41, 1585 (1978)

(31) A. Ali and F. Barreiro, Phys. Lett. 118B, 155 (1982); Nucl. Phys. B236, 269 (1984); D.G. Richards, W.J. Stirling and S.D. Ellis, Phys. Lett. 119B, 193 (1982); Nucl. Phys. B229, 317 (1983)

(32) B. Adeva et al. (MARK-J Collaboration), Phys. Rev. Lett. 50, 2051 (1983); ibid, 54, 1750 (1985); M. Althoff et al. (TASSO Collaboration), Zeit f. Phys. C6, 157 (1984); Ch. Berger et al. (PLUTO Collaboration), DESY report 85-039 (1985)

(33) Considerable confusion on the determination of $\alpha_s(Q^2)$ in e^+e^- annihilation experimental agalyses has prevailed in the past due to the neglect of finite terms in $O(\alpha_s)^2$, which numerically are important.

(34) Adeva et al. (MARK J Collaboration) (in ref. 32)

(35) W. Bartel et al. (JADE Collaboration), DESY report 86-086 (1986)

(36) J.G. Körner, G. Schierholz and J. Willrodt, Nucl. Phys. B185, 365 (1981)

(37) O. Nachtmann and A. Reiter, Zeit. f. Phys. C16, 45 (1982)

(38) G. Altarelli and G. Parisi, Nucl. Phys. B126, 298 (1977)

(39) G. Arnison et al. (UA1 Collaboration), Phys. Lett. 147B, 493 (1984)

(40) A. Ali, F. Barreiro and B. van Eijk, DESY report (in preparation)

(41) A. Ali, Zeit. f. Phys. C1, 25 (1979)

(42) A. Ali and E. Pietarinen, Nucl. Phys. B154, 519 (1979)

(43) L. Wolfenstein, Phys. Rev. Lett. 51, 1945 (1983)

(44) Despite considerable phasse space available the decay modes $c \to s\ell^+\nu_e$ and $b \to c\ell^-\bar{\nu}_e$, have been found to be dominated by K,K* and D,D*, respectively. For an experimental update see Gilchrese in ref. 5

(45) P.H. Gisparg, S.L. Glashow and M.B. Wise, Phys. Rev. Lett. 50, 1415 (1983)

(46) A.J. Buras, W. Slominski and H. Steger, Nucl. Phys. B245, 369 (1984), Nucl. Phys. B238, 529 (1984)

(47) M.A. Shifman and M.B. Voloshin, ITEP Reports 86-83, 86-84 (1986) and to be published

(48) L.B. Okun, V.I. Zacharov and B.M. Pontecorvo, Lett. Nuovo Cim. 13, 218 (1975); A. Pais and S.B. Treiman, Phys. Rev. D12, 244 (1975)

(49) M. Aguilar-Benitez et al. (Particle Data Group), Phys. Lett. 170B (1986)

(50) The values for P_d and P_s are suggested by the compilation of data, mostly from e^+e^- experiments. See, for example, D. Saxon, in proceedings of the European Physical Society Meeting on High Energy Physics, Bari, Italy (

(51) T. Schaad et al. (MARK II Collaboration), Phys. Lett. 160B, 188 (1985)

(52) H. Albrecht et al. (ARGUS Collaboration), DESY report 86/120 (1986)

(53) G. Arnison et al. (UA1 Collaboration), to be published; K. Eggert, in 'New Particles 1985', Conference proceedings University of Wisconsin, Madison, U.S.A. (1985)

(54) R. Barlow, Proceedings of the XX Recontre de Moriond, "Heavy Quarks, Flavour Mixing and CP violation" (La Plagne, France, 1985) p. 187; W. Bartel et al. (JADE Collaboration), Phys. Lett. 146B, 437 (1984); I.I. Bigi, Phys. Lett. 155B, 125 (1985)

(55) A. Ali and F. Barreiro, Zeit. f. Phys. C30, 635 (1986)

(56) A.I. Sanda, Phys. Rev. Lett. 55, 2653 (1985); J.M. Gerard et al., Phys. Lett. 140B, 349 (1984); Nucl. Phys. B253, 93 (1985); M. Dugan, B. Grinstein and L. Hall, Nucl. Phys. B255, 413 (1985)

(57) A.B. Carter and A.I. Sanda, Phys. Rev. Lett. 45, 952 (1980); Phys. Rev. D23, 1567 (1981); L.-L. Chau and H.-Y. Cheng, Phys. Lett. 165B, 429 (1985); M. Bander, D. Silverman and A. Soni, Phys. Rev. Lett. 43, 242 (1979); Dan-di Wu (in ref. 17); Bigi and Sanda (in ref. 17)